CAMERA-BASED FLUX DENSITY MEASUREMENTS SUPPORTED BY RAYTRACING SIMULATIONS

Christian Raeder, Utami Schmidt, Reiner Buck
Deutsches Zentrum für Luft- und Raumfahrt

Fundamental principle: Determination of reflection properties using the scanning method

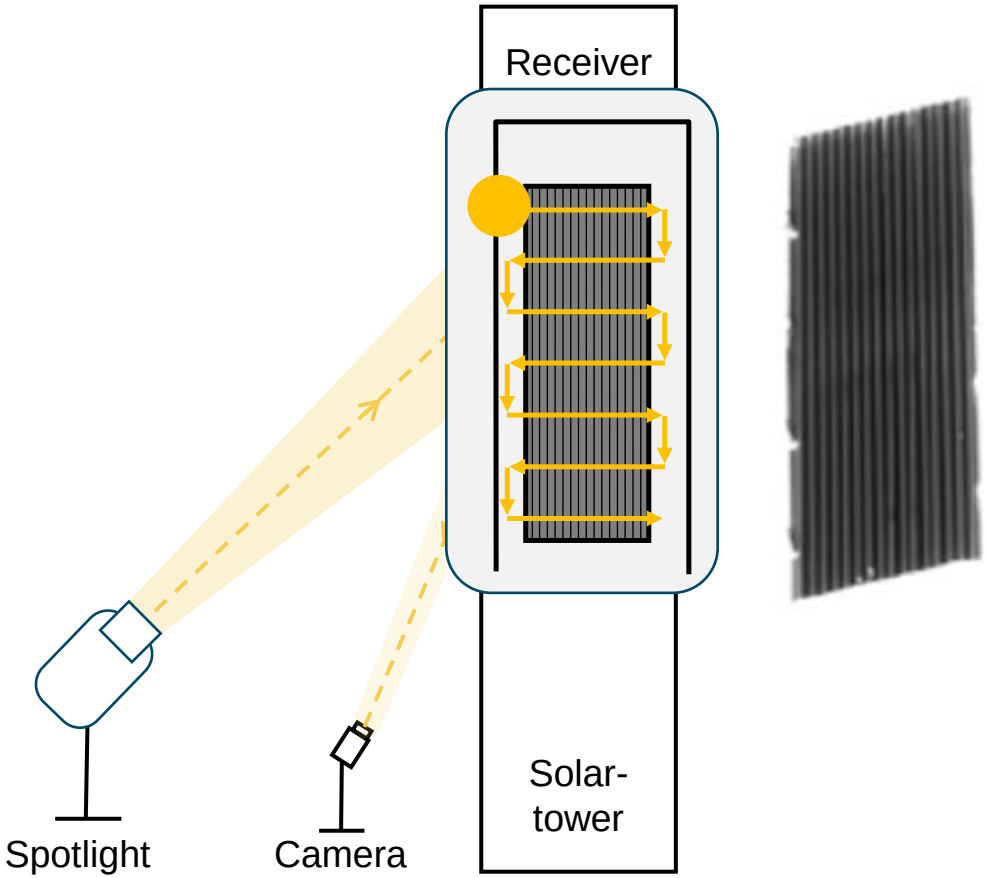

Scanning procedure

- Performed at night
- Meandering irradiation cycle
- High-frequency continuous shooting (greyscale images)
- Composition of a maximum image

Result

- **Reflection properties** of the absorber (with regard to an irradiation direction)

Image processing steps:
An overview of the rectification process

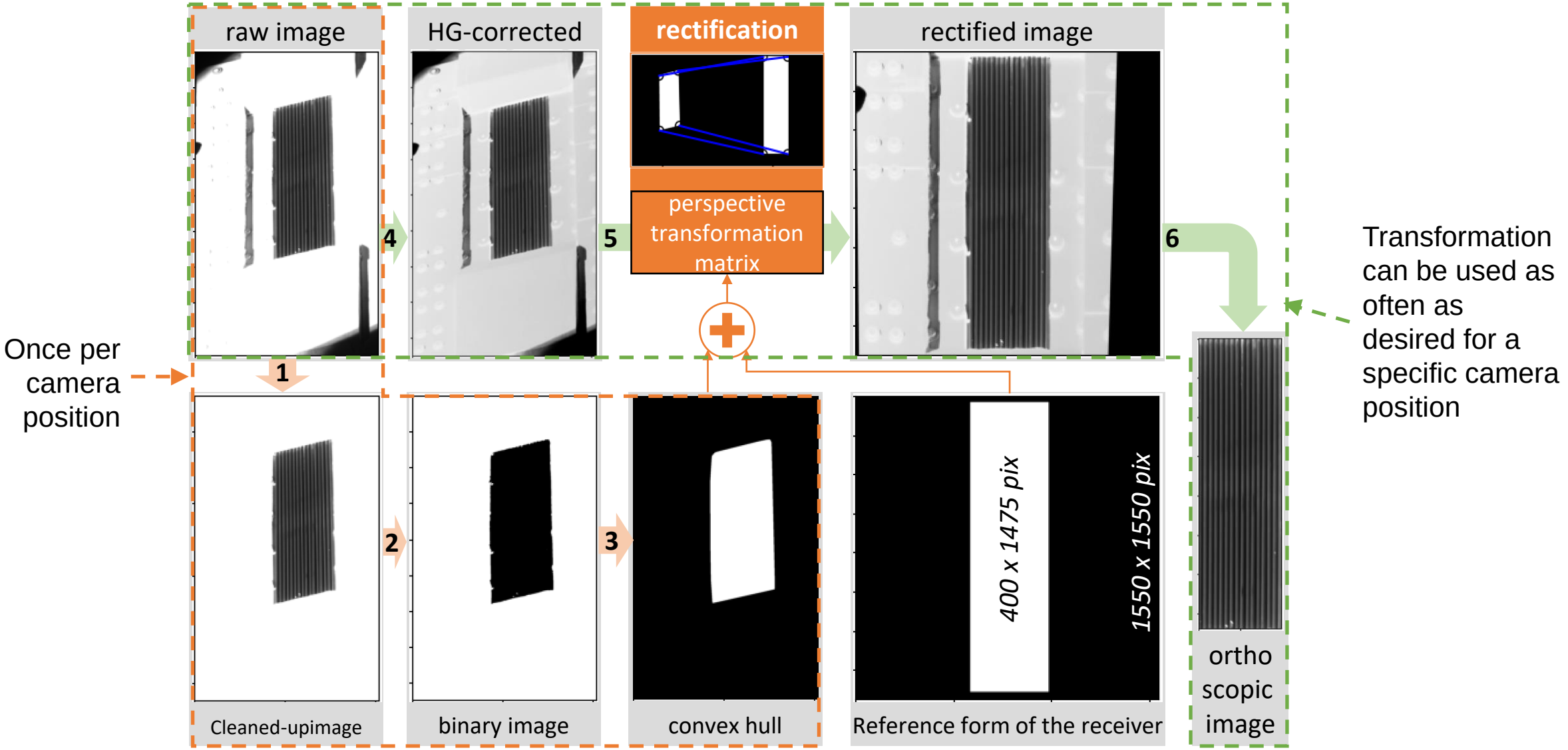

Image processing steps:
Dynamic ROI determination & mean images

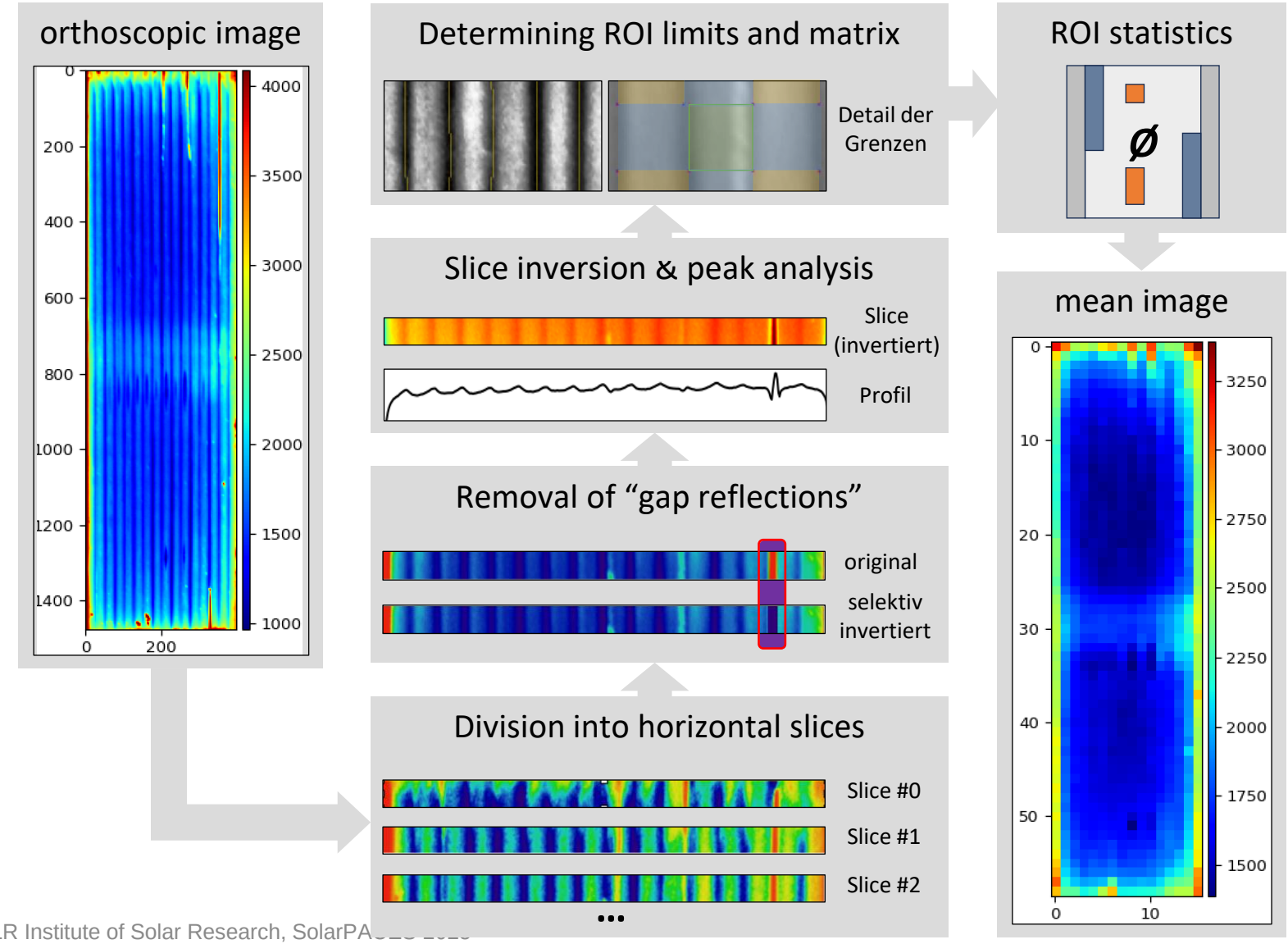

Fundamental principle: Optical flux density measurement using the scanning method

mean image [-]

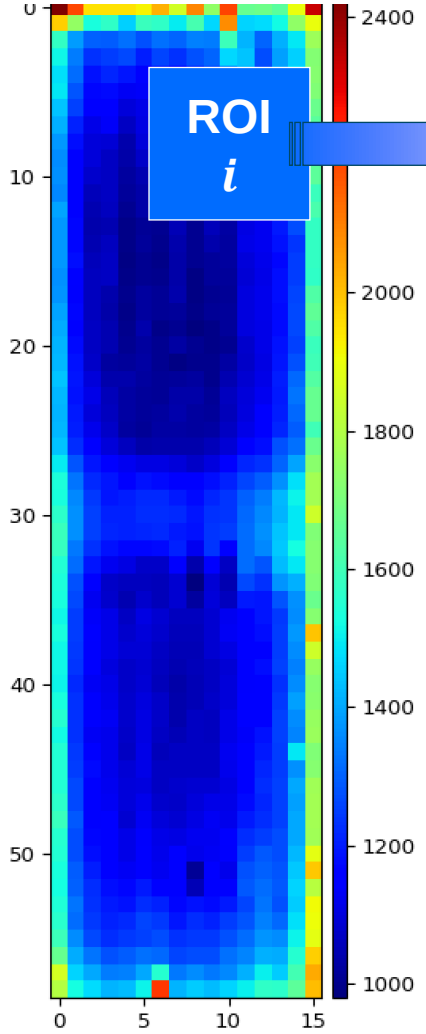

Main formula for calculating flux density [OFF19]

$$E_i = g_i \cdot \underbrace{\frac{1}{\sum_j \left(\rho_{i,j}/\bar{\rho} \cdot x_{i,j}\right)}}_{\text{correction}} \cdot \underbrace{\frac{1}{\bar{\rho} \cdot k}}_{\text{calibration}} \left[\frac{\mathrm{W}}{\mathrm{m}^2}\right]$$

- E_i: flux density distribution
- g_i: raw image (mean image)
- $\rho_{i,j}/\bar{\rho} \cdot x_{i,j}$: reflection correction
- directional composition

[OFF19]: M. Offergeld et al. 2019, doi: 10.1063/1.5117617

Measurement series:
Determination of directional composition - “Flux Fractions”

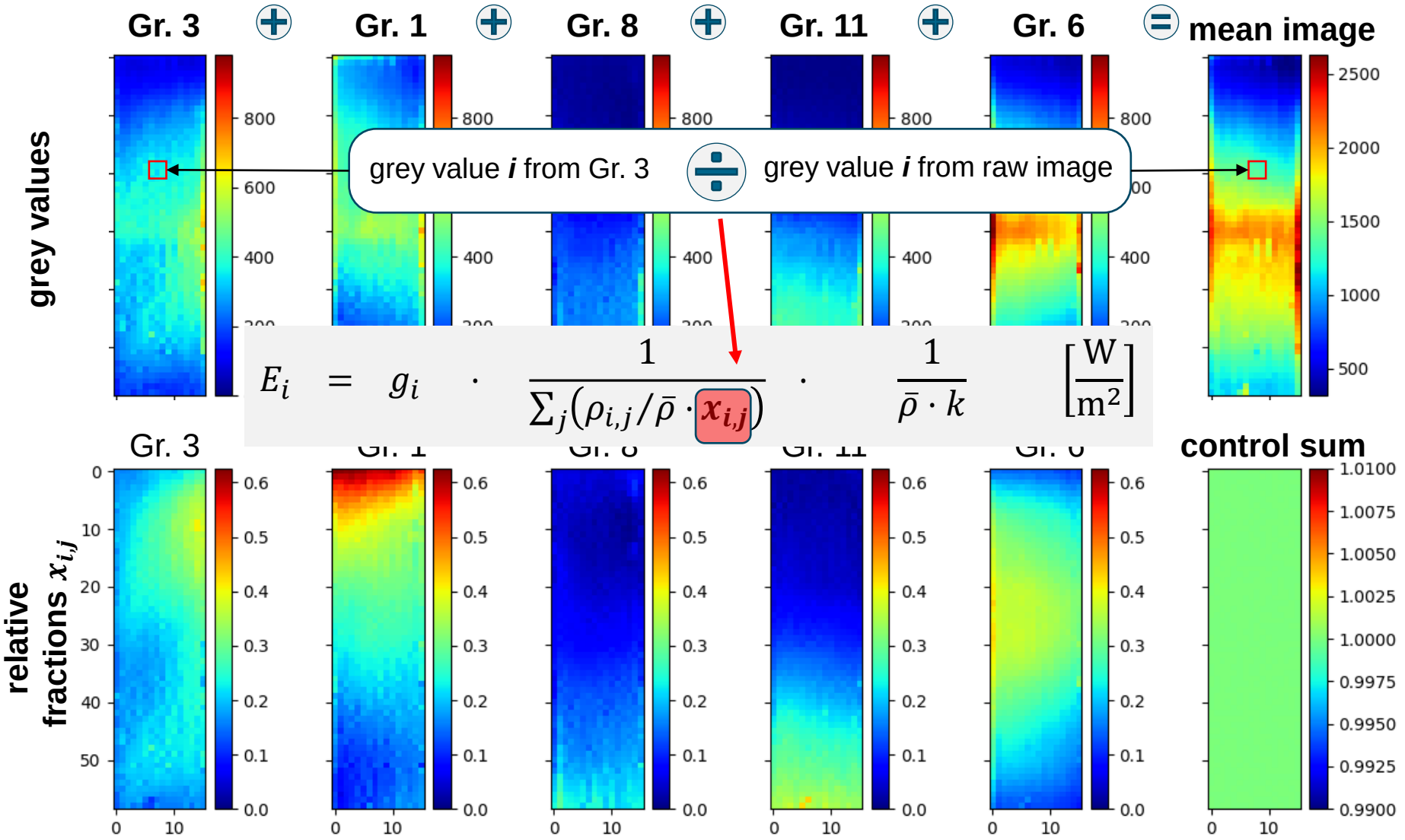

Flux density calculation - experimental data

$$E_i = g_i \cdot \frac{1}{\sum_j \left(\rho_{i,j} / \bar{\rho} \cdot x_{i,j} \right)} \cdot \frac{1}{\bar{\rho} \cdot k} \quad \left[\frac{\mathrm{W}}{\mathrm{m}^2} \right]$$

flux density distribution

in W/m²

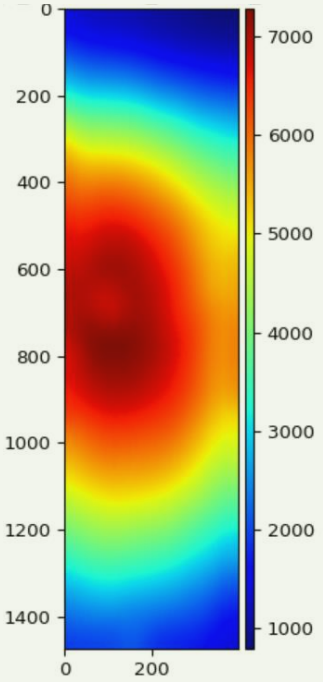

grey value image

DNI-corrected raw image V2 (5 heliostats from 5 groups)

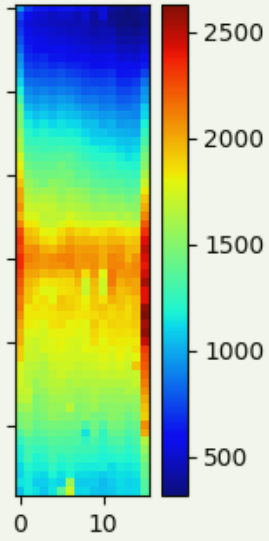

relative reflectivity (groups 1, 3, 6, 8, 11)

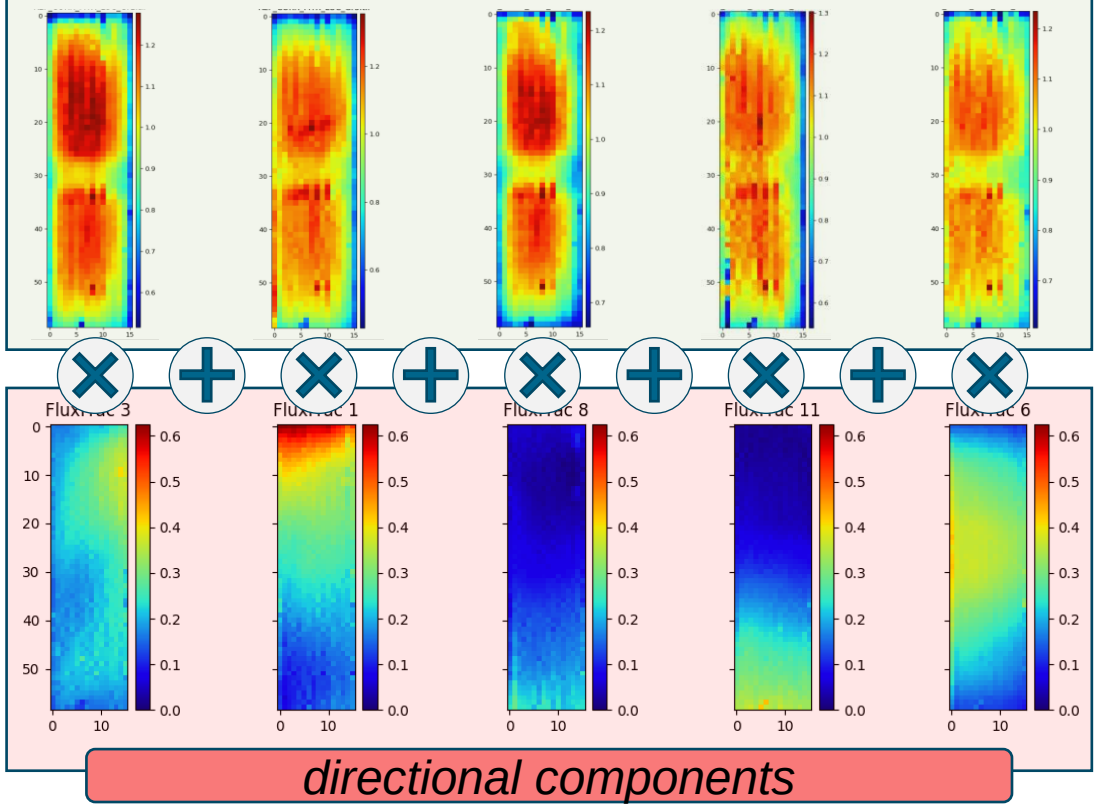

directional components

calibration

Factor from focus shift:
3,15 W/m²

×

Exposure time focus shift:
250 µs

÷

Exposure time defocusing V2:
280 µs

Measurement series:
Determination of directional composition

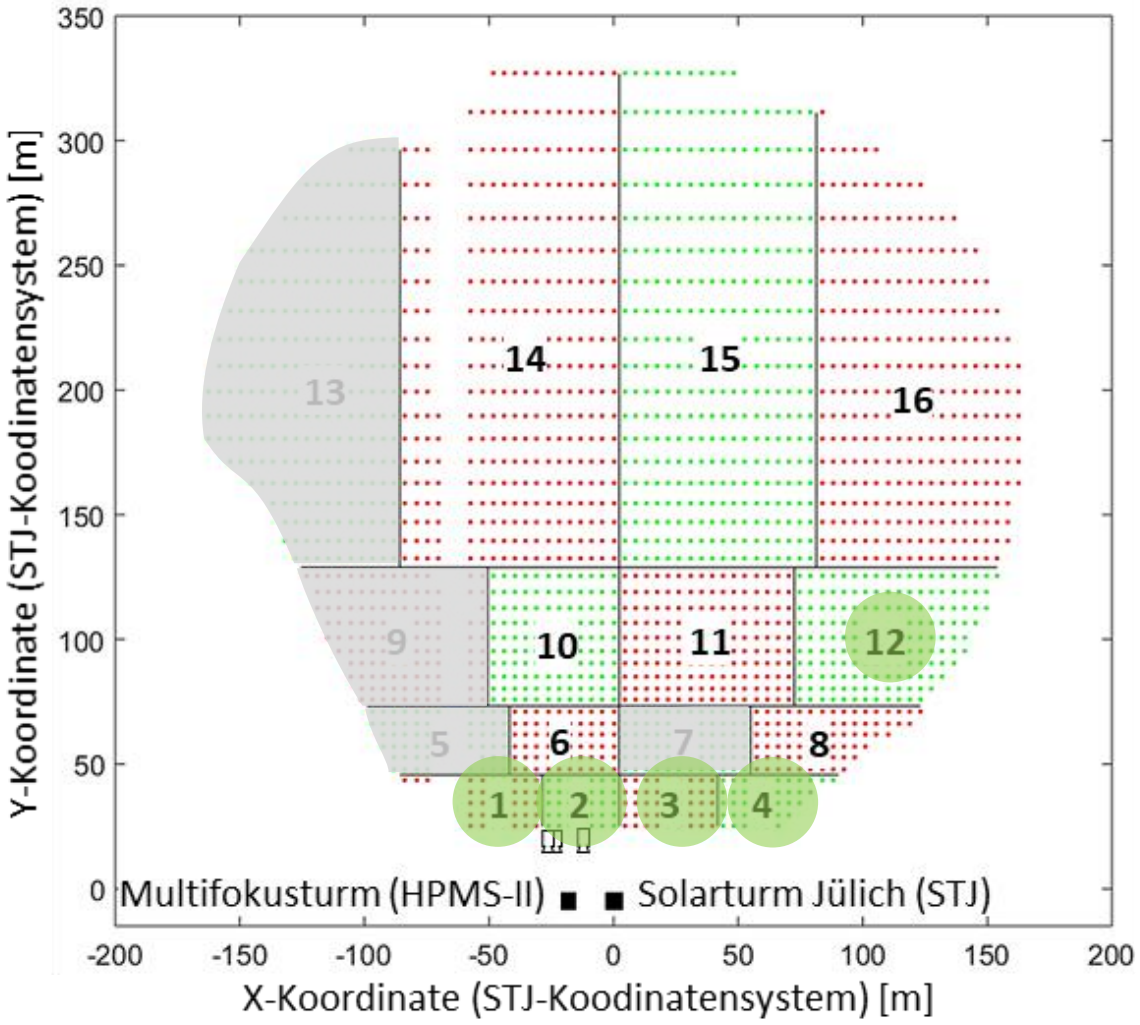

Versuch Nr.	Genutzte Heliostat-gruppen
1	1, 2, 3, 4, 12
2	1, 3, 6, 8, 11
3	1, 12, 14, 15, 16
4	2, 3, 6, 10, 14
5	1, 3, 8, 11, 15
6	4, 8, 10, 12, 16
7	1, 2, 6, 14, 16
8	4, 10, 11, 12, 15

Measurement series:
Determination of directional composition

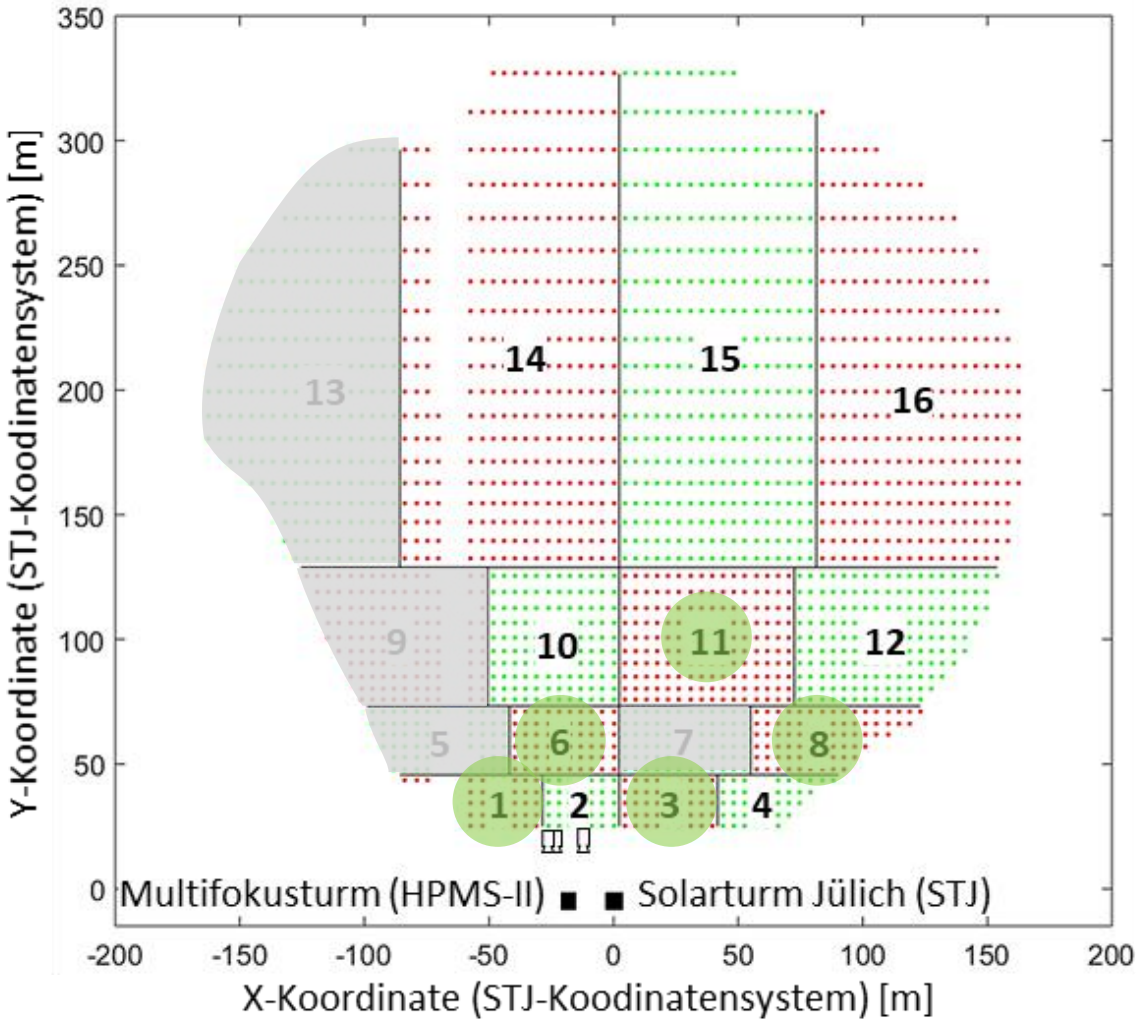

Versuch Nr.	Genutzte Heliostat-gruppen
1	1, 2, 3, 4, 12
2	1, 3, 6, 8, 11
3	1, 12, 14, 15, 16
4	2, 3, 6, 10, 14
5	1, 3, 8, 11, 15
6	4, 8, 10, 12, 16
7	1, 2, 6, 14, 16
8	4, 10, 11, 12, 15

Measurement series:
Determination of directional composition

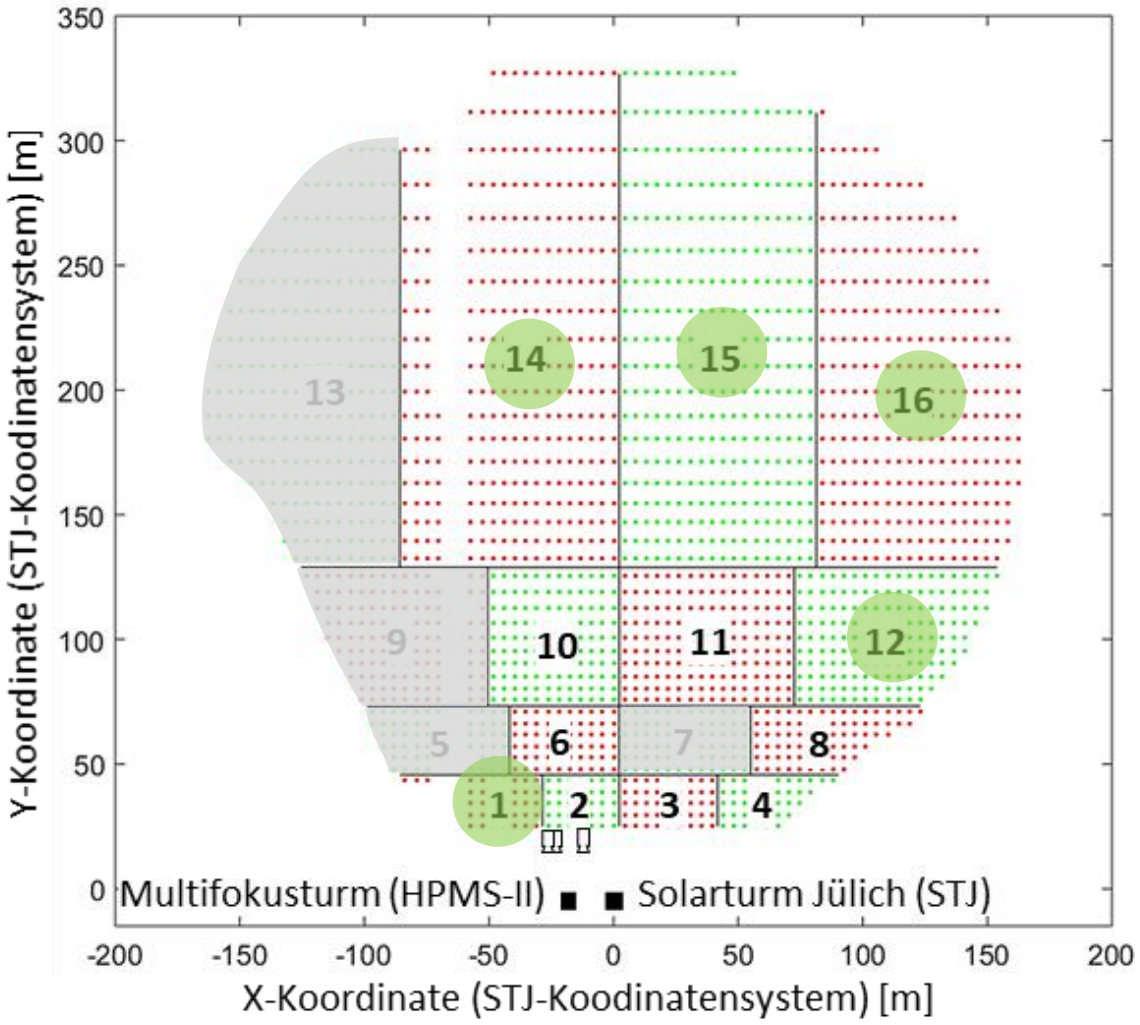

Versuch Nr.	Genutzte Heliostat-gruppen
1	1, 2, 3, 4, 12
2	1, 3, 6, 8, 11
3	1, 12, 14, 15, 16
4	2, 3, 6, 10, 14
5	1, 3, 8, 11, 15
6	4, 8, 10, 12, 16
7	1, 2, 6, 14, 16
8	4, 10, 11, 12, 15

Measurement series:
Determination of directional composition

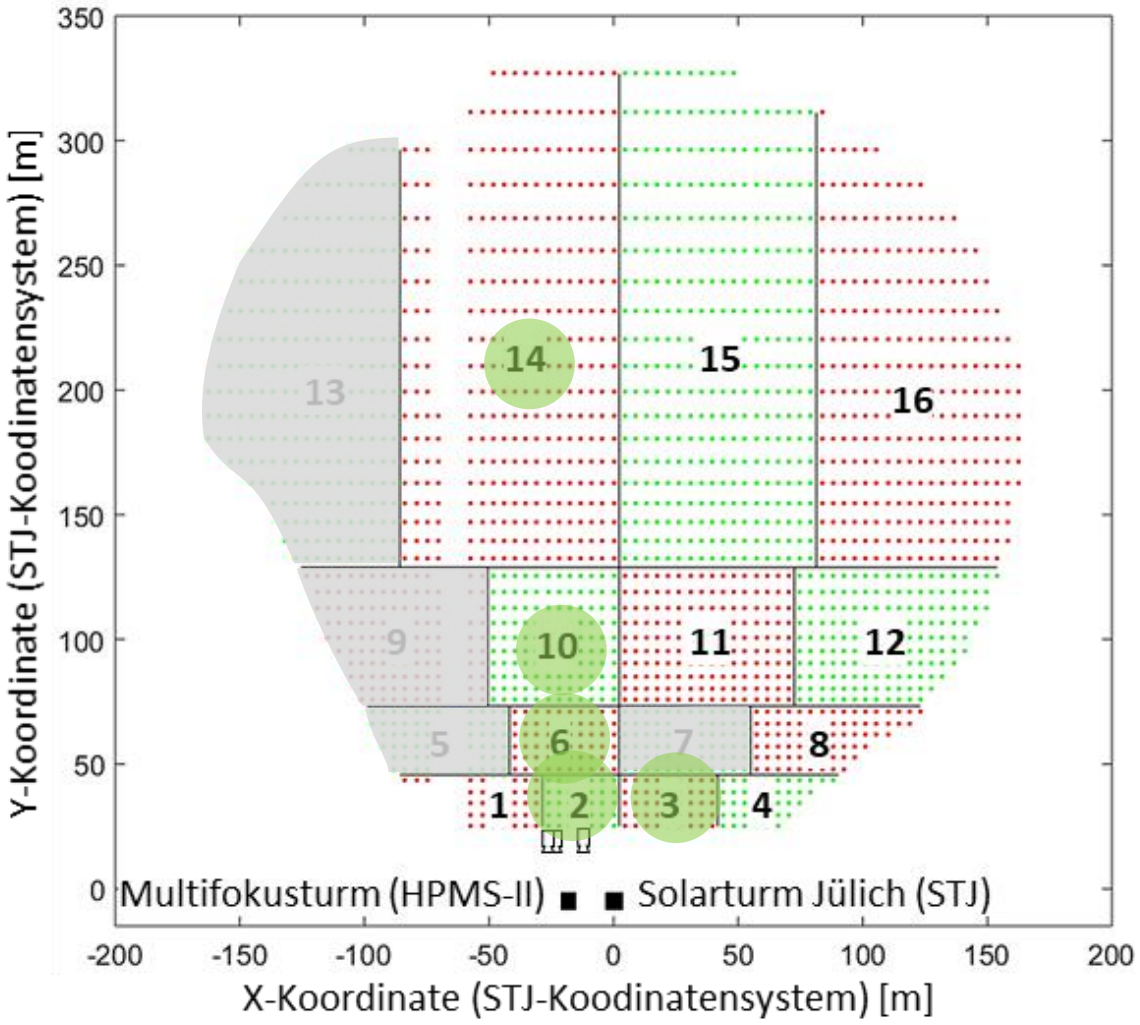

Versuch Nr.	Genutzte Heliostat-gruppen
1	1, 2, 3, 4, 12
2	1, 3, 6, 8, 11
3	1, 12, 14, 15, 16
4	2, 3, 6, 10, 14
5	1, 3, 8, 11, 15
6	4, 8, 10, 12, 16
7	1, 2, 6, 14, 16
8	4, 10, 11, 12, 15

Measurement series:
Determination of directional composition

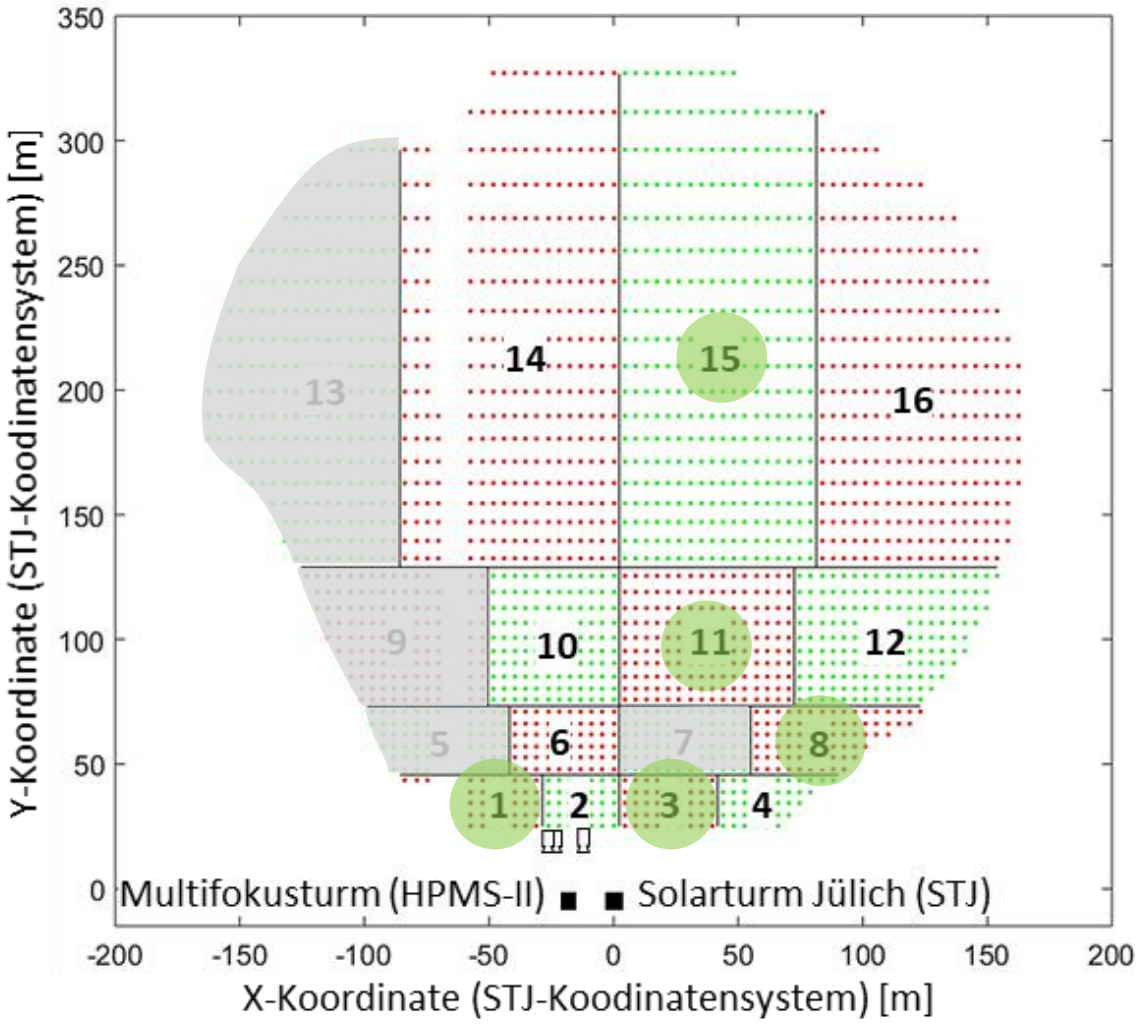

Versuch Nr.	Genutzte Heliostat-gruppen
1	1, 2, 3, 4, 12
2	1, 3, 6, 8, 11
3	1, 12, 14, 15, 16
4	2, 3, 6, 10, 14
5	1, 3, 8, 11, 15
6	4, 8, 10, 12, 16
7	1, 2, 6, 14, 16
8	4, 10, 11, 12, 15

Measurement series:
Determination of directional composition

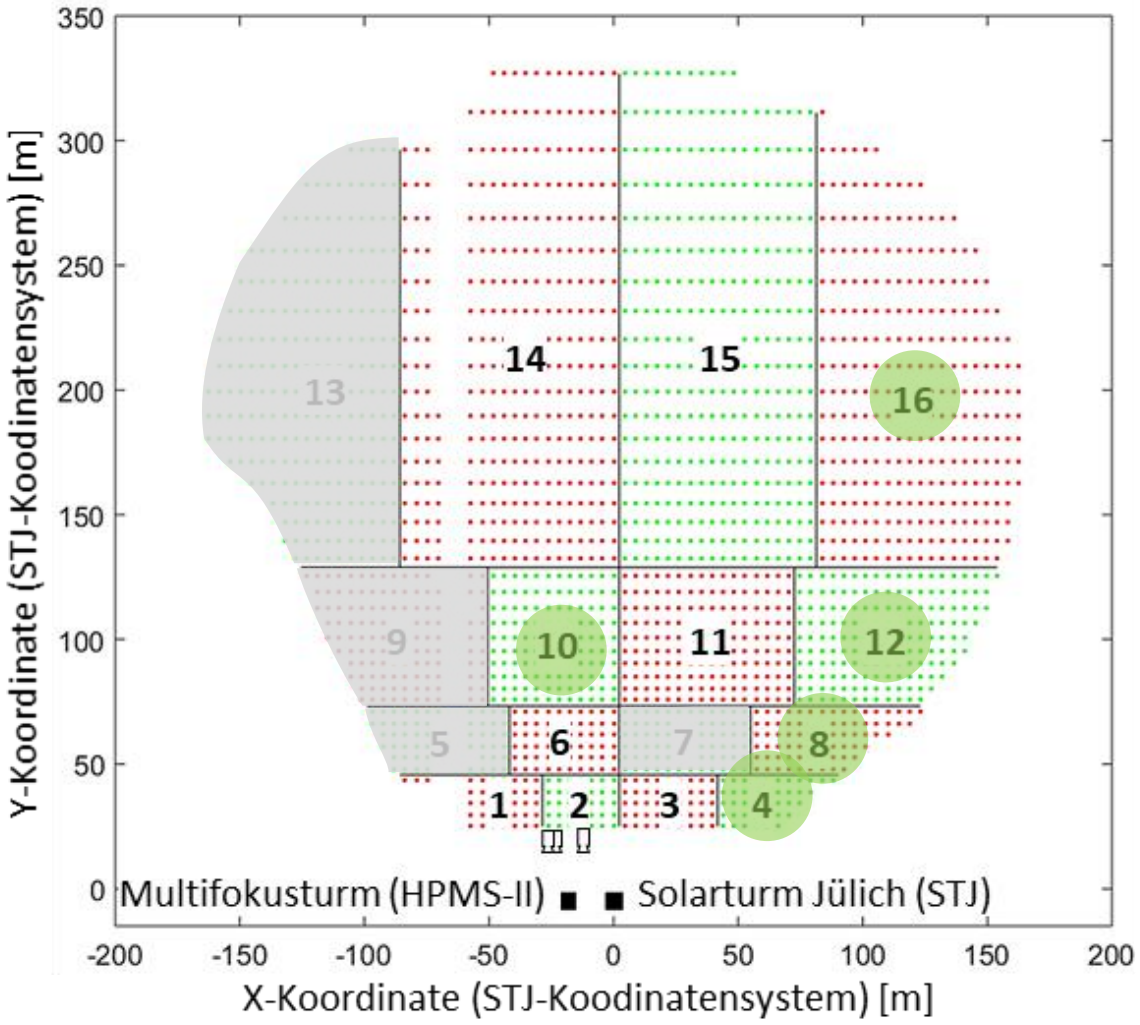

Versuch Nr.	Genutzte Heliostat-gruppen
1	1, 2, 3, 4, 12
2	1, 3, 6, 8, 11
3	1, 12, 14, 15, 16
4	2, 3, 6, 10, 14
5	1, 3, 8, 11, 15
6	4, 8, 10, 12, 16
7	1, 2, 6, 14, 16
8	4, 10, 11, 12, 15

Measurement series:
Determination of directional composition

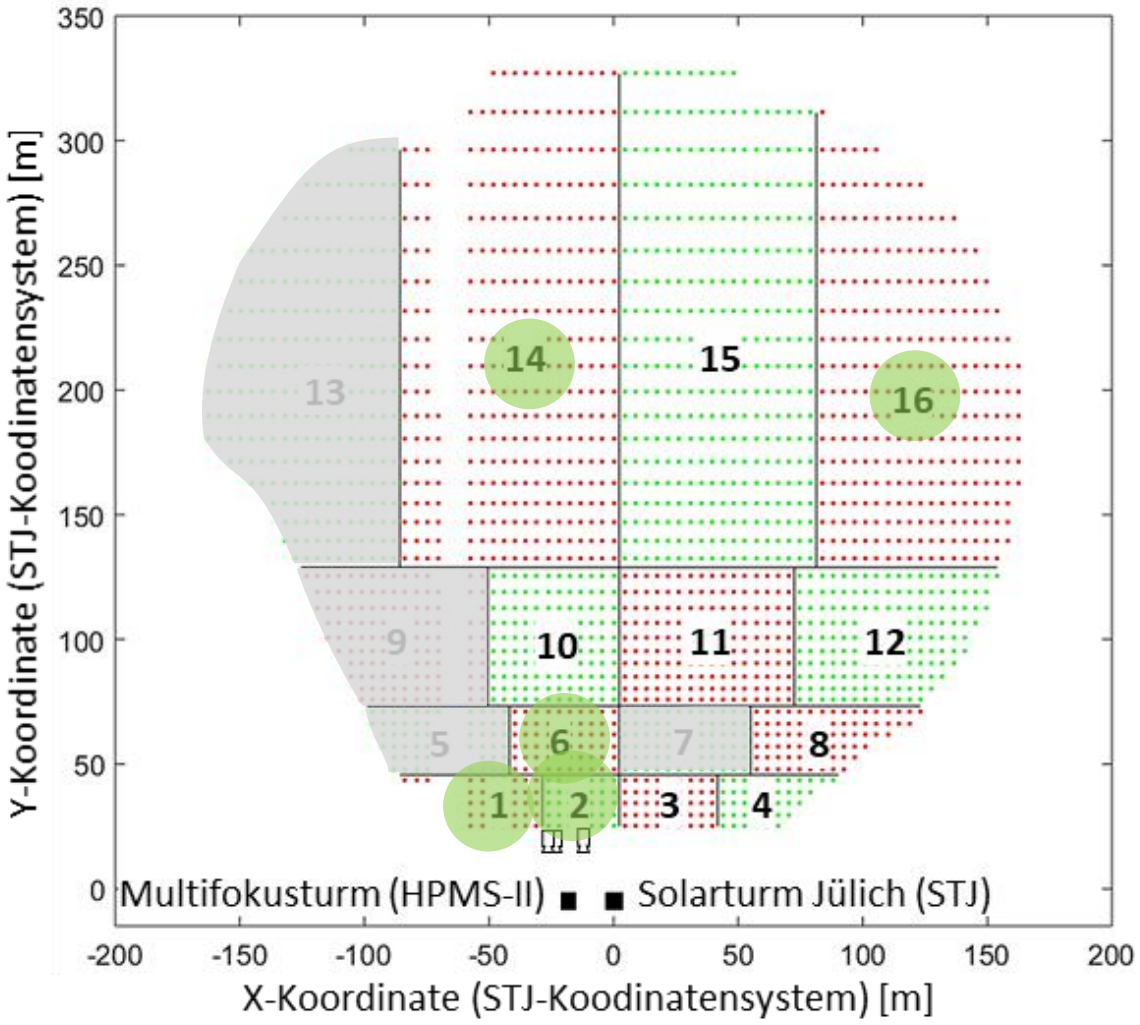

Versuch Nr.	Genutzte Heliostat-gruppen
1	1, 2, 3, 4, 12
2	1, 3, 6, 8, 11
3	1, 12, 14, 15, 16
4	2, 3, 6, 10, 14
5	1, 3, 8, 11, 15
6	4, 8, 10, 12, 16
7	1, 2, 6, 14, 16
8	4, 10, 11, 12, 15

Measurement series:
Determination of directional composition

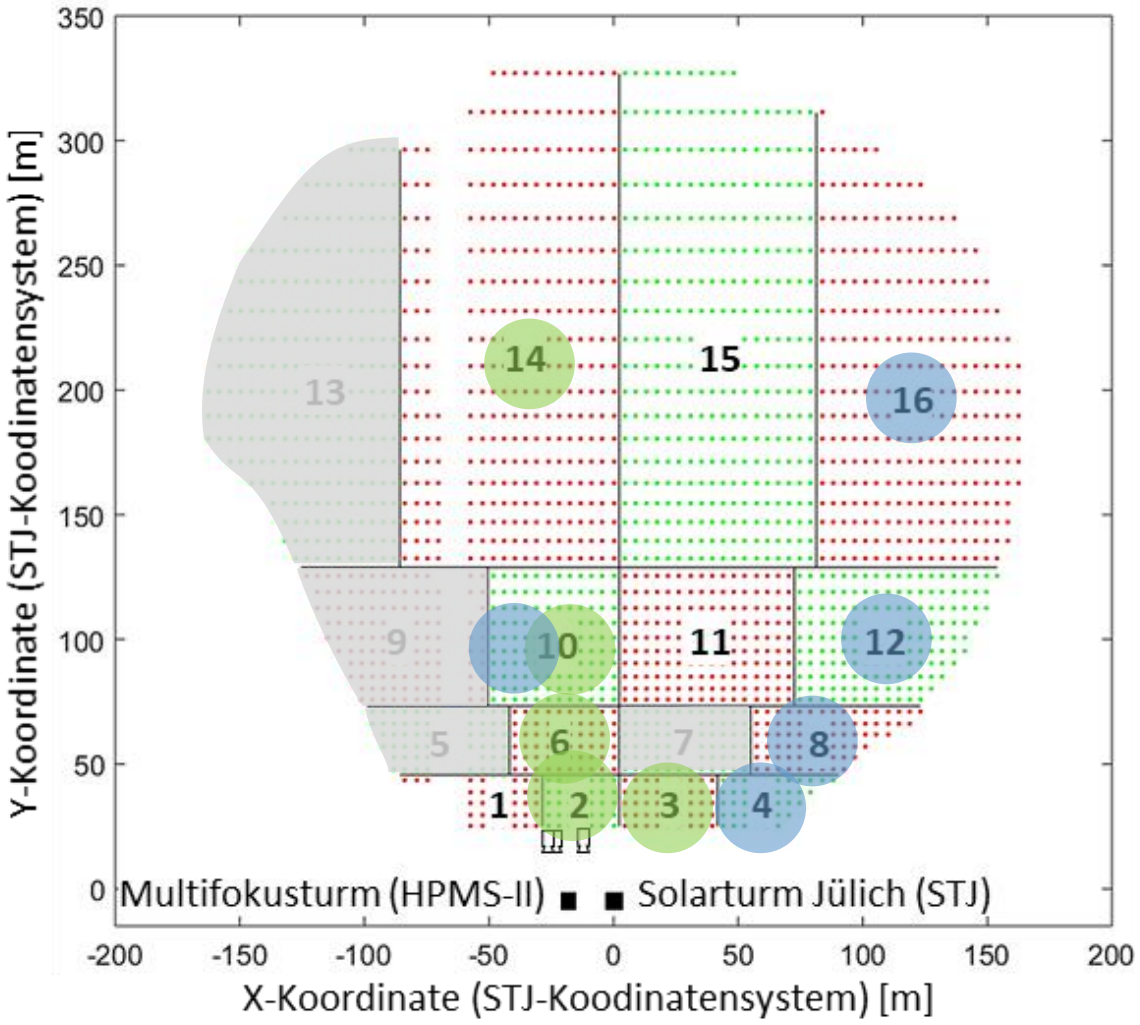

Versuch Nr.	Genutzte Heliostat-gruppen
1	1, 2, 3, 4, 12
2	1, 3, 6, 8, 11
3	1, 12, 14, 15, 16
4	2, 3, 6, 10, 14
5	1, 3, 8, 11, 15
6	4, 8, 10, 12, 16
7	1, 2, 6, 14, 16
8	4, 10, 11, 12, 15

Calculated flux density distributions and corresponding max images of the night scans

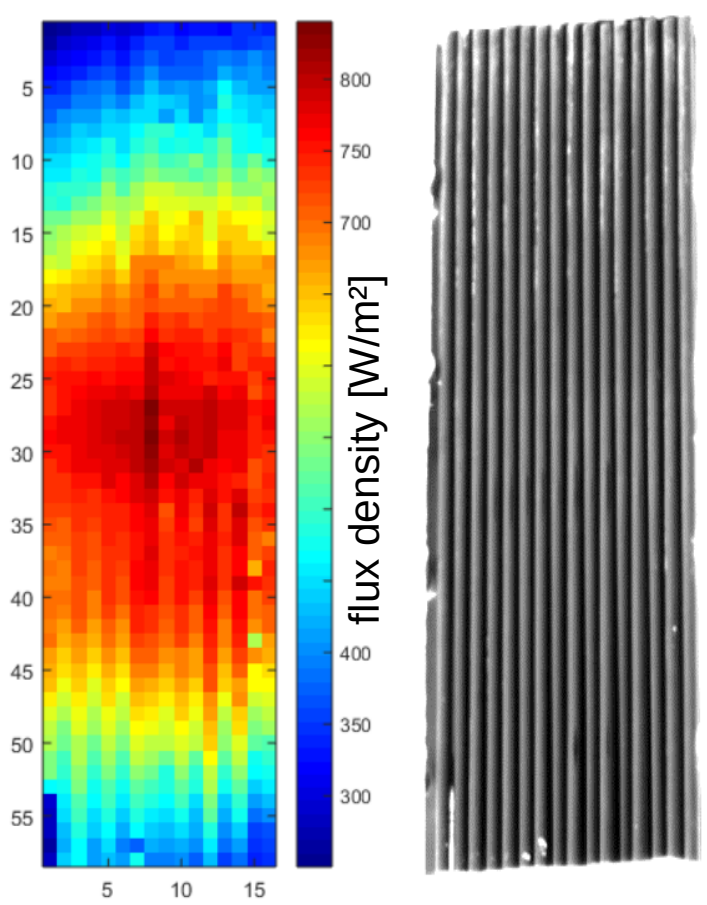

group 11

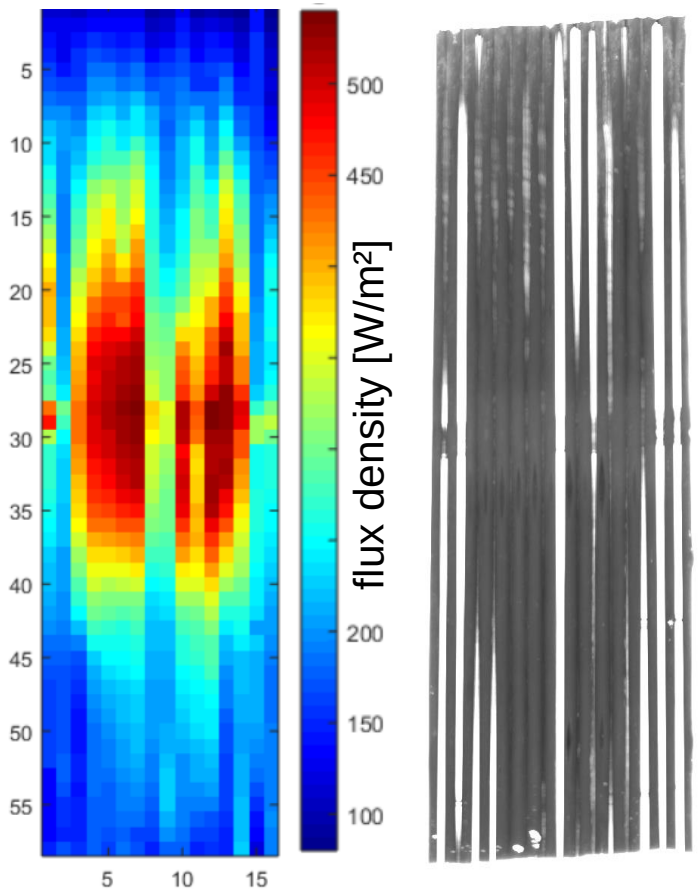

group 6

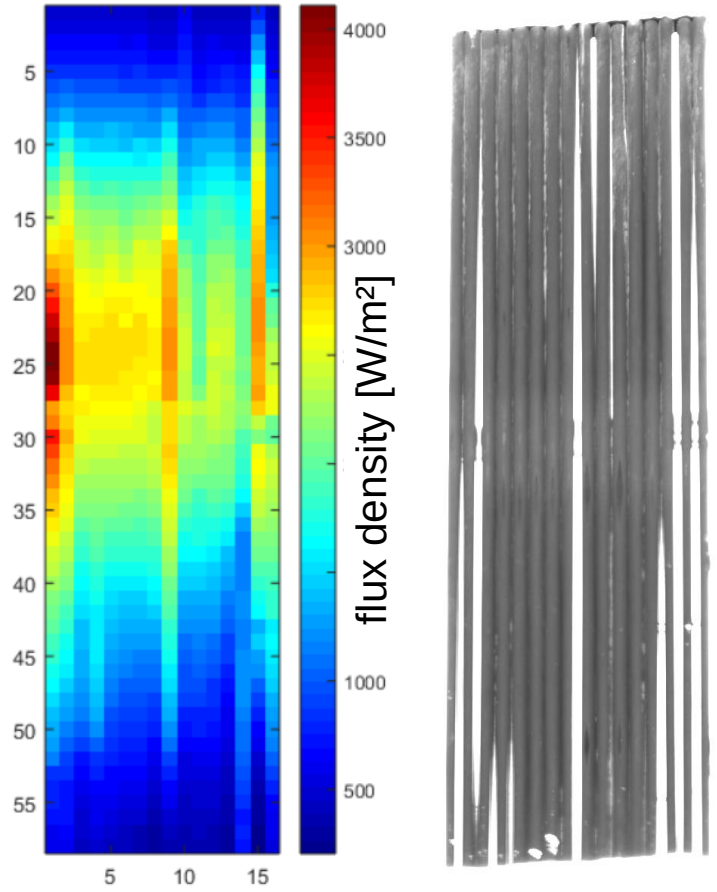

group 10

Raytracing with SPRAY: Modeling and evaluation

Triggers for reflections:
tube deformations
→ **Modeling in SPRAY**

Accuracy of simulation:
Angle-dependent reflection properties
→ **Measurement of samples in a lab-reflectometer**

Evaluation of results:
Determination of reflection and absorption components
→ **Component-wise evaluation & visualisation**

Evaluation & visualisation
→ **Additional correction term**

ANSYS-Model of the HPMS-II Receiver

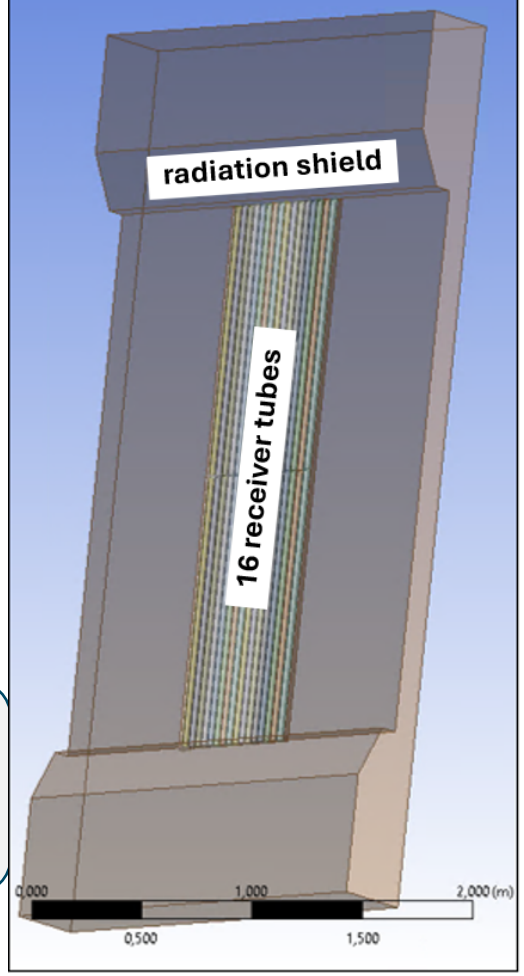

top view of receiver tubes and evaluation surfaces

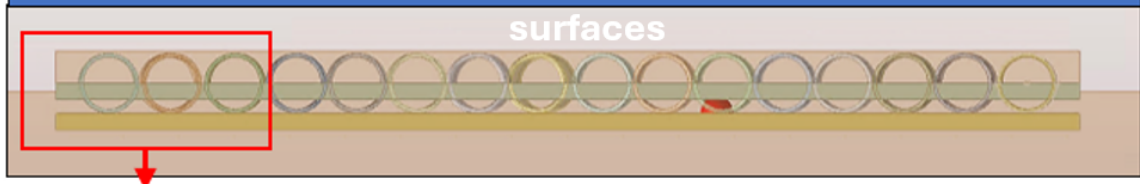

schematic arrangement of the evaluation areas

- Component 1: back of the tubes (C1.back)
- Component 2: front of the tubes (C1.front)
- Component 3: central evaluation plane (C3)
- Component 4: radiation shield (C2)
- Component 5: frontal evaluation plane (C4)

scheme for splitting incoming radiation

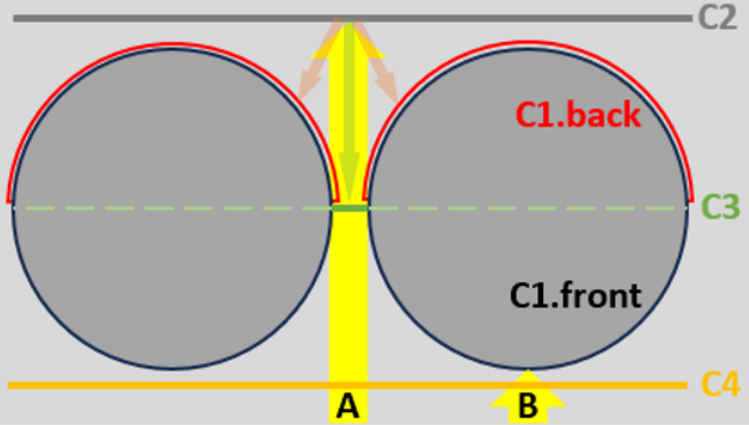

Case A:
Irradiation: C2
- Reflection: **C1.back** (energy input)
- Reflection: **C3** (direct reflection)

Case B:
Irradion: C1.front
- Reflection: C4

Use of SPRAY ray tracing simulation: Results – visualisation example

image Group 2
(AC33, Cam.-Pos. 1)

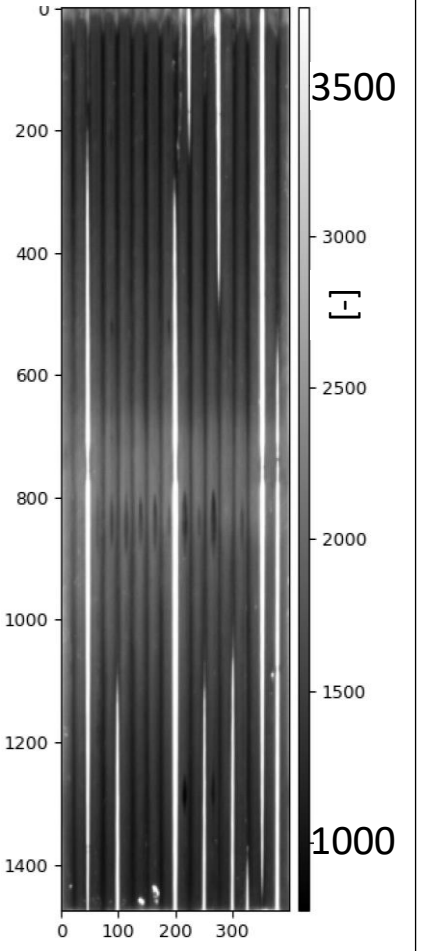

Simulation Group 2 – Comp. 3 (**C3**):
Reflected flux density between pipes

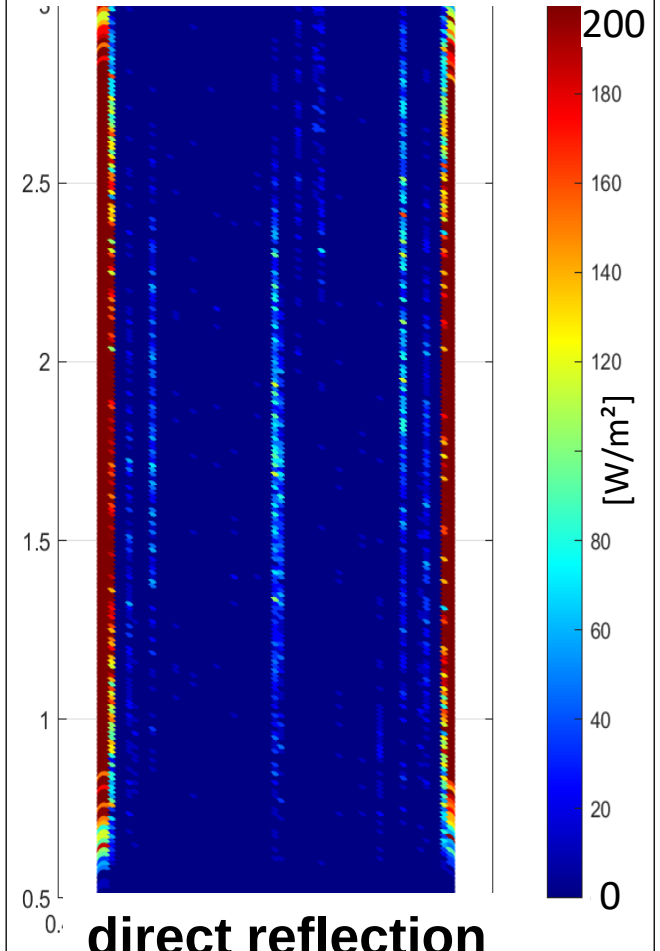

direct reflection

Simulation Group 2 – Component 1 (**C1.back**):
Absorbed flux density on the rear sides of the pipes

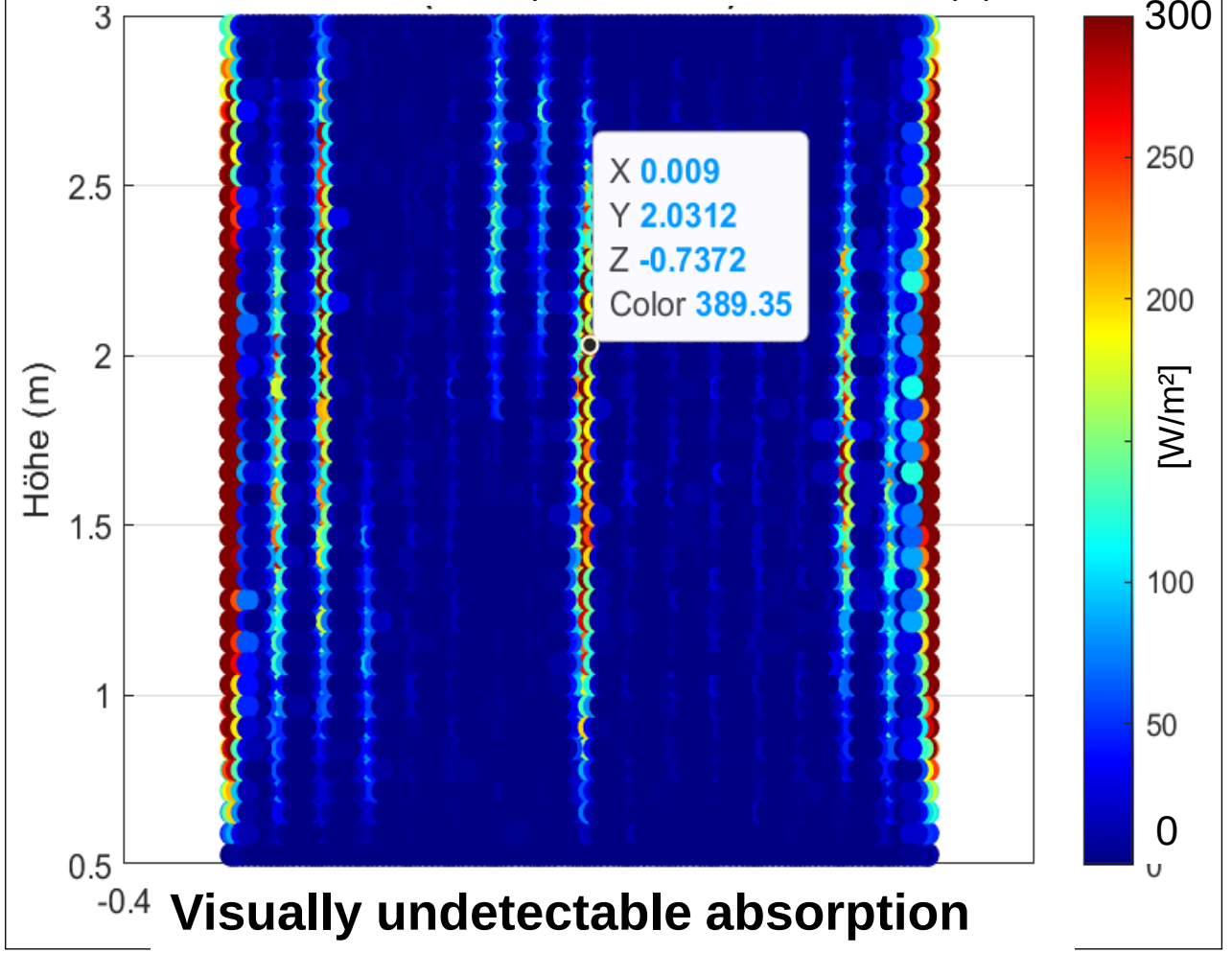

Visually undetectable absorption

Use of the SPRAY ray tracing simulation: Results – Additional correction term

$$E_i = g_i \cdot \frac{1}{\sum_j \left(\rho_{i,j}/\bar{\rho} \cdot x_{i,j}\right)} \cdot \frac{1}{\bar{\rho} \cdot k} \quad \left[\frac{\mathrm{W}}{\mathrm{m}^2}\right]$$

$$E_i = g_i \cdot \frac{1}{\sum_j \left(\rho_{i,j}/\bar{\rho} \cdot x_{i,j}\right)} \cdot \frac{1}{\bar{\rho} \cdot k} + \sum_j \bar{E}_{R,j} \quad \left[\frac{\mathrm{W}}{\mathrm{m}^2}\right]$$

additive correction term:
Sum of average flux density of the participating HG

groups 2, 3, 6, 10, 14 → **225 W/m²**
→ **approx. 5%** of the average flux density of the optical FDM

groups 4, 8, 10, 12, 16 → **84 W/m²**
→ **approx. 3%** of the average flux density of the optical FDM

Average flux density on the rear side of the tubes [W/m²]	invisible absorbed flux density component [%]	HG
25.4	1.8	1
53.0	3.4	2
17.8	1.4	3
3.4	0.5	4
59.2	3.8	6
225 W/m²	0.8	8
55.5	3.8	10
26.4	2.1	11
8.7	1.1	12
39.6	3.7	14
27.2	2.7	15
10.5	1.5	16

Thank You!

Utami Schmidt, Reiner Buck,
Volker Rasing, Sergio Díaz, Allen Charly, Judith Zöller, Matthias Glinka, Lukas Jäger,...

…and many more